Tissue-Specific Gene Delivery via Nanoparticle Coating

Todd J. Harris[a,§], **Jordan J. Green**[b,§], **Peter W. Fung**[a], **Robert Langer**[c], **Daniel G. Anderson**[c,*], and **Sangeeta N. Bhatia**[a,d,*]

[a]Harvard-MIT Division of Health Sciences and Technology, Cambridge, Massachusetts 02139, USA

[b]Department of Biomedical Engineering, Johns Hopkins University School of Medicine, Baltimore, Maryland 21205, USA

[c]The David H. Koch Institute for Integrative Cancer Research, Massachusetts Institute of Technology, Cambridge, Massachusetts 02139, USA

[d]MIT Electrical Engineering and Computer Science/Brigham & Women's Hospital, Boston, MA & Howard Hughes Medical Institute, Cambridge, Massachusetts 02139, USA

Abstract

The use of biomaterials for gene delivery can potentially avoid many of the safety concerns with viral gene delivery. However, the efficacy of polymeric gene delivery methods is low, particularly *in vivo*. One significant concern is that the interior and exterior composition of polymeric gene delivery nanoparticles are often coupled, with a single polymer backbone governing all functions from biophysical properties of the polymer/DNA particle to DNA condensation and release. In this work we develop electrostatically adsorbed poly(glutamic acid)-based peptide coatings to alter the exterior composition of a core gene delivery particle and thereby affect tissue-specificity of gene delivery function *in vivo*. We find that with all coating formulations tested, the coatings reduce potential toxicity associated with uncoated cationic gene delivery nanoparticles following systemic injection. Particles coated with a low 2.5:1 peptide:DNA weight ratio (w/w) form large 2 micron sized particles in the presence of serum that can facilitate specific gene delivery to the liver. The same particles coated at a higher 20:1 w/w form small 200 nm particles in the presence of serum that can facilitate specific gene delivery to the spleen and bone marrow. Thus, variations in nanoparticle peptide coating density can alter the tissue-specificity of gene delivery in vivo.

1. Introduction

Genetic medicine has the potential to benefit many diseases ranging from cancer [1,2] to hemophilia [3]. A key hurdle to its clinical application is the lack of safe and effective delivery systems [4,5]. There are many barriers to gene delivery including cellular barriers (intracellular uptake, endosomal escape, DNA release, and nuclear uptake) and extracellular barriers (avoidance of particle clearance mechanisms, targeting to specific tissues and/or cells of

interest, and protection of DNA from degradation) [6,7]. Significant advances have been made in our group [8] and other groups [9–11] in creating polymeric nanoparticles that have high efficacy *in vitro*, in some cases rivaling viruses. Yet, these particles do not necessarily have high efficacy *in vivo* in desired tissues, especially following systemic administration.

One main challenge is that cationic nanoparticles are generally found to have increased delivery *in vitro* due to electrostatic associations between the positively charged particle and the negatively charged cell surface. However, *in vivo*, this same positive charge promotes electrostatic association with negatively charged serum proteins, along with subsequent opsonization and clearance of the particle [12]. Neutralizing the charge of the cationic nanoparticles can potentially allow for improved biodistribution following intravenously administration. For example, PEGylation and/or covalent attachment of transferrin ligands to polyethylenimine (PEI) can increase gene expression of PEI/DNA particles in distant tumors [13,14]. However, covalently modifying cationic gene delivery polymers to reduce charge or add targeting ligands can also potentially decrease gene delivery efficacy [15,16].

As an alternative approach, physical electrostatic coating methods can also be used to modify nanoparticles either by adding positively charged or negatively charged coats [17,18]. Recently, it was demonstrated that electrostatically coated poly(beta-amino ester) nanoparticles can facilitate ligand-mediated gene delivery *in vitro* [19]. In this work, negatively charged polyglutamic acid-based peptides containing the Arginine-Glycine-Aspartic Acid (RGD) ligand were coated onto positively charged nanoparticles and shown to increase *in vitro* gene delivery to endothelial cells compared to scrambled sequence coated particles that contained RDG instead of RGD. While this approach looks promising, it is unclear how various electrostatic coatings affect gene delivery *in vivo*, as is required for the treatment of organ specific diseases like hemophilia.

One of the more promising polymers for gene delivery is degradable poly(beta-amino ester), 1,3-diaminopentane-terminated poly(5-amino-1-pentanol-co-1,4-butanediol diacrylate) (referred to here as C32-117, Figure 1). This polymer was previously demonstrated to be effective at *in vitro* gene delivery and *in vivo* delivery at levels orders of magnitude higher than polyethylenimine (PEI) [8,20–22]. This polymer functions by binding to and protecting DNA from degradation, enabling efficient cellular uptake, and enabling subsequent intracellular endosomal escape [22]. However, as with many nanoparticle formulations, its systemic use *in vivo* is limited due to poor biodistribution and lack of tissue-specific targeting [20].

Here, we develop nanoparticle coatings that direct tissue-specific delivery of polymeric gene vehicles *in vivo*. In particular, we show that specific tissue delivery can be enhanced by tuning the biophysical properties of coated nanoparticles.

2. Materials and Methods

Unless otherwise stated all reagents were purchased from Sigma-Aldrich and all reactions were performed at room temperature.

2.1 Polymer synthesis

C32-117 was synthesized as described previously [8,20]. Briefly, acrylate-terminated poly(5-amino-1-pentanol-co-1,4-butanediol diacrylate) (C32), was synthesized by the addition of 5-amino-1-pentanol (Sigma-Aldrich, St. Louis, MO, USA) to 1,4-butanediol diacrylate (Scientific Polymer Products Inc., Ontario, NY, USA) at a 1.2:1 molar ratio of diacrylate monomer to amine monomer. Polymerization took place in a 20 mL Teflon-lined screw cap glass vial under magnetic stirring at 90°C for 24 hours. To form C32-117, 9.1 g of THF (Sigma-Aldrich) was then added to 5 g of freshly synthesized C32, vortexed well, and then this solution

was transferred to an opaque 100 mL glass bottle. Ten mmols of "117" (1,3-diaminopentane, Sigma-Aldrich) was next dissolved in 40 mL of THF. This solution was then added to the C32/THF solution and stirred magnetically overnight at room temperature. Polymers were precipitated by repeat washes with 3 volumes of diethyl ether and centrifugation, followed by drying overnight under vacuum. Dried polymer was dissolved in DMSO (Sigma-Aldrich) to 100 mg/mL and stored at −20 °C until use.

2.2 Peptide synthesis

The peptides used in this work were synthesized by the MIT Biopolymers core and their purity was verified by HPLC and mass spectrometry. The poly-E peptide sequence is NH2-GK (TAMRA)- GGGGGGEEEEEEEEEEEEEEEEE-CONH2. The poly-E-cat peptide sequence is NH2-GK(TAMRA)-GdPdLGdVdRG-GGGGGGEEEEEEEEEEEEEEEE-CONH2.

2.3 Nanoparticle synthesis and transfection

To form nanoparticles, DNA, C32-117, and peptide were each first dissolved in 25 mM sodium acetate buffer solution at pH 5.2 (NaAc buffer), which was prepared by diluting a 3 M stock (Sigma-Aldrich). For each preparation, 60 μL of polymer/NaAc solution (30 mg/mL) was then added to 60 μL of DNA/NaAc solution (1 mg/mL) in a 1.5 mL eppendorf tube and vortexed for ten seconds (30:1 w/w ratio of polymer to DNA). After a five minute incubation at room temperature to allow for nanoparticle self-assembly, 60 μL of peptide solution (0, 2.5, 5, 10 or 20 mg/mL) was added, mixed well, and left to incubate at room temperature for 5 minutes. Finally, 60 μL of PBS with 20% glucose was added and 200 μL of nanoparticles (50 μg DNA) was immediately injected intravenously via the tail vein or measured for biophysical characterization. In some of the injected formulations Alexa-680 labeled DNA was spiked in at a 1:10 w/w dilution for tracking DNA accumulation.

2.4 DNA and DNA labeling

DNA plasmids, pCMV-LUC and pEGFP-N1 (Elim Biopharmaceuticals, Hayward, CA) were used as received. For DNA accumulation experiments, Alexa-680 labeled DNA was also prepared by labeling pCMV-LUC. Free thiols were coupled to the DNA backbone using the FastTag reagent kit (Vector) according to the manufacturer's protocol. Alexa-680 maleimide (Invitrogen) was attached to the free thiols and the labeled DNA was purified on a G50 gel filtration column.

2.5 Bioluminescence imaging

Swiss Webster mice were intravenously injected with 50 μg of complexed and coated pCMV-LUC plasmid DNA in 200 μL intravenously. After 6 hrs, animals were injected i.p. with 4.5 mg of luciferin (Promega) in 300 μL and the level of luciferase gene expression was quantified using an IVIS whole mouse bioluminescence imaging system (Xenogen). Animals were imaged on their abdomen and back and ROIs were drawn around the spleen from a posterior view and the liver, femurs, and lungs from an anterior view.

2.6 Sizing and zeta potential

For sizing measurements 1 volume of coated or uncoated nanoparticles was added to 7 volumes of PBS containing 12% fetal bovine serum (FBS). Dynamic light scattering was used to determine the hydrodynamic intensity-weighted effective diameter of particles at various time points for 3 separately formulated solutions using a Nano-ZS90 (Malvern). For zeta potential measurements 1 volume of coated or uncoated nanoparticles was added to 7 volumes of PBS with or without 12% FBS. Zeta potential measurements were taken for 3 separately formulated solutions using a Nano-ZS90.

2.7 Erythrocyte aggregation assay

Fresh mouse blood was isolated and added to an equal volume of buffer containing PBS and 10 mM EDTA. Erythrocytes were pelleted by centrifugation, washed multiple times in PBS, and diluted 4-fold. To one volume of fresh erythrocytes was added one volume of coated or uncoated C32-117 nanoparticles. Solutions were incubated for 1 hr at 37 °C and diluted 40-fold into a 96-well plate for phase contrast imaging.

2.8 Histology

Mouse livers were isolated 6 hrs post injection with 2.5:1 w/w poly-E coated nanoparticles and were frozen in OCT compound for sectioning. Liver sections were fixed with cold acetone, washed in PBS and incubated in blocking buffer (PBS + 12% FBS) for 20 minutes. Sections were then washed and incubated with rat anti-F480 IGG or rat anti-CD31 IGG (BD Pharmingen) and rabbit anti-GFP IGG (ABD Serotec) for 24 hrs. Sections were washed and a secondary stain of alexa 546-labeled goat anti-rat IGG (Invitrogen) and alexa 647-labeled goat anti-rabbit IGG (Invitrogen) was applied for 1 hour. The antibodies were washed and the sections were stained with 0.0001% Hoechst for 20 min prior to mounting with Fluor mount-G (Southern Biotech). Liver sections were imaged on an inverted fluorescence microscope mounted with a CCD camera (Nikon Ellipse TE200 and CoolSnap-HQ). UV, Texas red, and Cy5 filter cubes (Chroma) were used to image nuclear, antigen, and GFP stains respectively.

2.9 Hepatocyte isolation

Hepatocytes were isolated from mice 6 hrs after injection with 2.5:1 w/w poly-E coated particles using a modified procedure developed in rats [23]. Hepatocytes were purified from the rest of the cell population with multiple centrifugal spins at 500 rpm in KRB buffer. Cells were resuspended in FACs buffer (PBS with 1% FBS) and analyzed by flow cytometry.

2.10 Bone marrow isolation and labeling

Bone marrow cells were isolated from mice 6 hrs after injection with 20:1 w/w poly-E-cat coated particles. The bone marrow was titrated from the femur and tibia bones with RPMI media (GIBCO) containing 5% FBS using a 28 gauge syringe and passed through a 70 μm cell strainer. Cells were centrifuged at 1000 rpm and resuspended in 1 mL of RBC lysis buffer. After a 5 min incubation cells were diluted in RPMI media with 10% serum and centrifuged at 1260 RPMs for 5 min at 4 °C. Cells were washed 1x with FACs buffer and resuspended in 1 mL of blocking solution made up of FACs buffer containing a 1:200 dilution of anti-mouse FcγIII/II (Pharminogen). Cells were incubated for 5 minutes and 100 μL aliquots were removed and added to 100 μL of biotin-labeled primary Gigs diluted 1:100 in FACs buffer (antimouse IGG control, TER-119, CD5, CD4, CD8, CD3, CD45R, GR1, and CdllB – Pharminogen). After a 20 min incubation, each aliquot was washed and incubated with a 1:400 dilution of streptavidin-PE-Cy5 (Pharminogen) in FACs buffer. Cells were washed and resuspended in FACs buffer for flow cytometry.

2.11 Flow cytometry

Isolated hepatocytes and bone marrow cells were analyzed on a BD LSR II flow cytometer with a 488 nm excitation source and a 530/30 bandpass filter for GFP expression and 570/36 bandpass filter for autofluorescence (PE) detection, as well as a 405 nm excitation source and a 670/14 bandpass filter for PE-Cy5 detection. The percentage of GFP positive cells was determined by gating non-fluorescent cells isolated from an untreated animal on a 2-D scatter plot with axes of autofluorescence (PE) and GFP. Fold enhancement of GFP expression for bone marrow cells was determined by dividing the percentage of GFP positive cells for a maker-positive subset over the percentage of GFP positive cells in the whole blood marrow population. Analysis and gating was performed using FlowJo software.

2.12 Statistics

Two-way ANOVA and Bonferroni post-tests were used to calculate statistical significance of biophysical properties including particle size (versus coating type and incubation time) and zeta potential (versus coating type and presence of serum) as compared to uncoated nanoparticles. Two-way ANOVA Bonferroni post-tests were also used to calculate significance for log transformed luciferase transfection RLUs to compare coated particles to uncoated particles among each organ type In all cases * = p<0.05, ** = p<0.01, *** = p<0.001. All error bars show mean +/− standard deviation.

3. Results and Discussion

3.1 Formulation of coated particles

We hypothesized that the biodistribution and gene delivery efficacy of polymeric nanoparticles could be modified *in vivo* by tuning electrostatic peptide coatings of the particles. The gene delivery nanoparticles are prepared through self-assembly. First, a cationic polymer is complexed with anionic DNA to form positively charged nanoparticles. To improve *in vivo* delivery, we develop a second step where the polymeric nanoparticles are coated electrostatically. As the nanoparticles are positively charged, anionic peptides are used for coatings. The peptides used each consist of three components: a stretch of poly (glutamic acid) that provides the negative charge, a linker of polyglycine, and a terminal sequence that varies in charge and has the potential to alter particle biophysical properties and tissue distribution. The base peptide, composed of poly (glutamic acid) and polyglycine, was chosen as a coating material since it is made up of naturally occurring amino acids that carry anionic charge and has been shown as a useful coating material *in vitro* [24]. The coatings as well as the particles themselves are biodegradable via their amide and ester linkages respectively.

To observe how coatings change biophysical properties of the nanoparticles, and how these biophysical properties, in turn, tune tissue specific delivery, peptides were chosen that do not contain specific ligands. The two full peptide sequences used are NH2-GK(TAMRA)-GGGGGGEEEEEEEEEEEEEEEEE-CONH2 (poly-E) and NH2-GK(TAMRA)-GdPdLGdVdRG-GGGGGG-EEEEEEEEEEEEEEEEE-CONH2 (poly-E-cat). While the two terminal sequences of the peptides possess no known receptor specificity, they vary in charge, with poly-E-cat containing a cationic insert sequence not present in poly-E.

To form the coated particles, the negatively charged poly(glutamic acid) residues electrostatically coat the positively charged nanoparticle in aqueous solution. A description of the coating scheme used is shown in Figure 2. As this figure demonstrates, cationic polymeric nanoparticles composed of C32-117 and DNA were first formed at a ratio of 30:1 weight polymer to weight DNA (w/w). These positively charged particles were then coated by anionic peptides, either poly-E or poly-E-cat, at peptide weight ratios ranging from 2.5:1 to 20:1 weight peptide to weight DNA.

3.2 Biophysical properties

Variable coating density of the same particles with the same peptide were found to modulate both the size and surface potential of the resulting nanoparticle. For example, non-coated particles have a positive zeta potential in PBS that becomes negative when the particles are incubated in PBS containing 10% serum (Figure 3d). When peptide coatings are added to the particles, their zeta potentials change from strongly positive to weakly negative in PBS. However, in contrast to the uncoated particles, when the coated particles are added to PBS containing 10% serum, their zeta potential does not change further due to the presence of serum. Only uncoated nanoparticles differ in zeta potential by the presence or absence of serum.

Particle size is also dramatically changed by the presence and extent of peptide coating (Figure 3e). When added to PBS containing 10% serum, most particles quickly grew in size within the first 10 min, indicating interactions with serum proteins. For example, uncoated particles grew to ~400 nm in size and 5–10:1 w/w peptide coated particles grew to ~1 μm in size. Particles with low 2.5:1 w/w peptide coating aggregated the most, with size increasing for 50 min before leveling off at ~2.5 μm. Interestingly, particles with a high level of 20:1 w/w peptide coating did not aggregate in the presence of serum and maintained a small size of ~200 nm, approximately half the size of the uncoated particles. Thus, the density of peptide coating plays a leading role in altering the biophysical properties of the nanoparticles. Low coating leads to high instability in the presence of serum and micron sized particles, whereas high coating density leads to small, stable nanoparticles with resistance to aggregation.

3.3 Effects of peptide coating density on in vivo delivery

Differences in coating density alter not only biophysical properties of the particles, but their biodistribution as well. Whole mouse bioluminescence imaging was performed using tail-vein injections of 50 μg of pCMV-LUC plasmid DNA complexed with polymer C32-117 and used uncoated or coated with poly-E peptides ranging from 2.5:1 to 20:1 w/w. Uncoated nanoparticles were found to exhibit poor gene expression and half of the mice injected with uncoated particles died within minutes after injection. In contrast, none of the mice injected with coated nanoparticles (2.5:1–20:1 w/w) died. Thus, coating the particles with peptides is advantageous in reducing toxicity. To examine the potential causes of this lethality, uncoated and coated C32-117 nanoparticles were mixed with freshly isolated erythrocytes *in vitro* (Figure 3c). Whereas uncoated particles caused significant aggregation of erythrocytes, the same particles coated with a low 2.5:1 w/w coating density of poly-E did not have any effect with the erythrocytes. The *in vivo* results also mirror the *in situ* zeta potential results which demonstrated that the coated particles do not change zeta potential when added to serum proteins, but the uncoated particles have a dramatic change in surface charge when exposed to serum proteins. Thus, the coatings likely reduce lethality by reducing the aggregation and opsonization of the particles with blood components including erythrocytes and serum proteins [12].

Particle biodistribution and gene delivery efficacy as a function of coating density is shown in Figures 3a and 3b. A lower, non-lethal 25 μg DNA half dose of uncoated particles is used as the "no coat" control since the full uncoated 50 μg DNA dose, as previously mentioned, resulted in lethality. These results show that peptide coating can increase *in vivo* gene expression of an exogenous plasmid by more than 10-fold in the liver compared to uncoated particles, while maintaining low levels of expression in the spleen and femur bone marrow. These effects were dependent on the level of peptide coating density and *in situ* particle sizing measurements. Low poly-E coating (2.5:1 w/w), which led to the largest particles, was well tolerated in mice and showed significantly enhanced gene expression in the liver compared to uncoated particles. Relative luciferase expression in the liver with these coated particles was 100-fold higher than the expression levels in the lung, spleen, or bone marrow. Intermediate coating densities (5:1–10:1 w/w) resulted in ~1 μm sized particles and transfected liver higher than uncoated particles, but lower than 2.5:1 coated particles. These particles were similar to uncoated particles for delivery to lung, spleen, and bone marrow. On the other hand, 20:1 w/w poly-E coated particles that formed stable ~200 nm nanoparticles had low gene delivery at or below the level of uncoated particles in the lung, liver, spleen, and bone marrow.

While whole animal imaging showed high luciferase expression in the liver following tail-vein injection of 2.5:1 w/w poly-E coated C32-117/DNA particles, bioluminescence can't discern the cell types being transfected. Therefore, histological analysis was performed to determine these cell types. Transfections were performed with low density poly-E peptide coatings the

same as before, but DNA encoding green fluorescent protein was used instead of luciferase DNA. Six hours post-injection, high levels of gene expression were found in the liver (Figure 4). GFP staining was found throughout the liver and localized to the lining and periphery of both CD31 positive and CD31 negative vessels. Antibody staining also revealed that the GFP signal also co-localized with F4-80 positive Kupffer cells near the lining of these vessels. This coated particle delivery system may be useful for the delivery of therapeutic genes to the liver.

3.4 Effects of peptide sequence on in vivo delivery

While poly-E coated particles with a low 2.5:1 w/w coating density formed large, slightly negative particles that had specific delivery to the liver, higher 20:1 poly-E coating densities formed small ~200 nm particles that eliminated gene delivery to the liver and elsewhere. We hypothesized that alteration of the terminal sequence of poly-E peptides could modulate and improve gene delivery function for these highly coated particles. We tested peptides with other terminal sequence inserts and found one that provided a unique gene delivery profile to the bone marrow and spleen. Nanoparticles coated with this peptide, which we call poly-E-cat because it contains the cationic amino acid sequence G-dP-dL-G-dV-dR-G between the K (TAMRA) and the poly-E sequence, delivered luciferase to the spleen, spine, sternum, and femur of mice (Figure 5a).

Gene delivery to the spleen, spine, sternum, and femur was substantially higher when particles were coated with 20:1 w/w poly-E-cat peptides compared to 20:1 w/w poly-E. Regions of luminescence selected around the femur bones showed nearly 40-fold enhancement by poly-E-cat coated particles over poly-E coated particles and regions around the spleen showed nearly 30-fold enhancement (Figure 5b). Particles coated with either poly-E-cat or poly-E peptides had similar particle sizes of 150–200 nm when incubated with serum over time (Figure 5d). However, the zeta potential of particles coated with poly-E-cat peptides are neutrally charged in PBS, whereas poly-E coated particles are more negatively charged (Figure 5c). This neutralizing of the surface potential may play a role in the functional differences of these two particles. Similarly to 20:1 w/w poly-E coated particles, particles coated with 20:1 w/w poly-E-cat peptides were also well-tolerated in mice and did not aggregate freshly isolated erythrocytes (Figure 6).

To examine which cells are transfected in the bone marrow, we isolated bone marrow cells from the femur of a mouse 6 hrs after tail-vein injection of particles coated with 20:1 w/w poly-E-cat peptide. For these experiments GFP DNA was used instead of LUC DNA and flow cytometry was performed to quantify the positively transfected cells. Cells were labeled with markers to identify specific cell subtypes and the percentage of cells expressing GFP in each cell type was compared to the whole bone marrow cell population. Cells positive for the monocyte marker GR1 had nearly 40-fold enrichment of GFP expression over the whole cell population (Figure 5e). T-cells, in particular CD8 T-cells, were enriched nearly 25-fold. This enrichment corresponds to gene transfection of 1 in 204 GR-1 positive monocytes and 1 in 313 CD8 positive T-cells. While these levels of transfection may not be sufficient for delivery strategies that require transfection of the entire monocyte or T-cell populations, this technique could potentially be useful to deliver genes to a portion of cells, which would subsequently migrate to peripheral tissues and express protein. This level of targeting may also be adequate for use of these nanoparticles as genetic vaccines. Increased DNA doses and/or multiple injections of particles may further improve the number of transfected cells.

3.5 Discussion

Intravenously administered cationic polymeric particles have the capacity to deliver genes with high efficiency to the lung. However, depending on the polymer molecular weight and solution ionic strength, these particles can be toxic [25,26]. When injected intravenously, cationic

particles can aggregate with serum proteins, erythrocytes, and other blood components to form complexes that can embolize and accumulate in vascular beds of the lung [17,27,28]. Similarly, we observed the toxicity of the cationic gene delivery nanoparticles used in this study as uncoated 50 μg DNA doses caused death in 2 of 4 mice within minutes after injection. To investigate if accumulation in the lungs could have caused this toxicity, we performed repeat experiments with infrared fluorophore labeled DNA to track its distribution. These experiments show where DNA accumulates within a mouse, whereas the luciferase experiments show where DNA is specifically taken up intracellularly, transcribed, and then successfully expressed. Labeled DNA did accumulate in the lungs of mice intravenously injected with the same uncoated nanoparticles that caused lethality (Figure 7). This accumulation did not occur with the non-lethal peptide coated particles.

While the 20:1 w/w poly-E coated particles in serum were half the size of the uncoated particles in serum, the 2.5:1 w/w coated particles in serum rapidly increased in size. This increase is indicative of instability in serum and may be a problem for *in vivo* delivery. However, our *in vivo* delivery experiments show that these particles are well-tolerated by the mice and no adverse effects are observed. In contrast, the uncoated particles, which have a steady ~400 nm size in serum, caused lethal toxicity. Thus, the increase in size of the 2.5:1 coated particles does not appear problematic for liver directed delivery.

It has been reported that the addition of polyacrylic acid to cationic polyethylenimine/DNA particles increases gene expression to the lung [17]. The authors of this study suggest that novel structures might form between the tertiary complex composed of polyethylenimine, DNA, and polyacrylic acid that is more effective for delivery and more resistant toward serum proteins than the binary polyethylenimine/DNA complex. In our study, we hypothesized that the electrostatic adsorption of varying anionic poly-glutamic acid-based coatings may neutralize the surface potential of cationic nanoparticles, modulate *in vivo* delivery, and reduce toxicity. We coated C32-117 cationic polymeric nanoparticles with varying w/w ratios of anionic 16-mer poly (glutamic acid) peptides terminated in a short glycine sequence. The poly-E coating was found to reduce interactions with both erythrocytes and serum proteins in the blood. This likely was responsible for the reduction in toxicity.

While reductions in toxicity by the neutralization of nanoparticle surface potential could possibly be expected [29], improvements in liver directed delivery by partially coated particles was unexpected. Reports have shown that a targeting ligand, most often a sugar, is needed for liver delivery through a process of receptor-mediated endocytosis. For example, when injected via the portal vein, galactosylated smaller sized particles transfect liver cells more efficiently than larger sized or ungalactosylated particles [30]. Other work has similarly shown that although intravenous injection of PEGylated polystyrene nanoparticles results in poor delivery to the liver, delivery is significantly increased by using galactosylated nanoparticles. In addition, galactosylation of 50 nm particles increases delivery to liver hepatocytes from negligible to 30% of the injected dose and galactosylation of 140 nm particles increases delivery to liver Kupffer cells from negligible to up to 90% of the injected dose with low delivery to liver hepatocytes also occurring [31]. Finally, numerous reports have also shown that galactose can be used to guide polymeric gene delivery particles to hepatocytes via the asialoglycoprotein receptor (ASGPR) [32,33]. Thus, receptor-mediated endocytosis (usually via an attached sugar) seems key for liver-targeted delivery. Yet, when poly(beta-amino ester) nanoparticles, similar to those used in our study here are galactosylated, delivery to hepatocytes is not increased or made more specific [34]. Beyond the targeting sugar, research with liposomes has also shown size specificity of uptake. Kupffer cells take up 500 nm particles more quickly than smaller 80 nm particles and hepatocytes more efficiently internalize the smaller particles [35].

In the 20:1 w/w coated particulate system used here, the particles are large, do not have a targeting sugar, and achieve liver delivery through a simple intravenous route. Interaction between the peptide coating and blood components may alter the biophysical properties of these particles and steer delivery to the liver. This could occur by changing the size of the particles and/or by the adsorption of particular serum proteins that promote receptor-mediated uptake and gene delivery. For example, in vitro studies have indicated that adsorption of immunoglobulin G (IgG) and complement protein C3 to nanoparticles increases their uptake by Kupffer cells and incubation in serum increases hepatic uptake *in vivo* following liver perfusion [36].

Poly-E and poly-E-cat particles coated at 20:1 w/w were both found to be small and stable in the presence of serum, but only poly-E-cat coated particles had specific delivery to the spleen and bone marrow. Thus small changes to peptide coating sequences, especially terminal charge, can dramatically change tissue distribution, likely through specific binding to serum components or cell surfaces. We are currently investigating the mechanistic details of how the minor change in peptide sequence shown here can mediate these effects. While uncoated particles primarily delivered DNA to the lung, and often caused lethality, peptide coated particles were found to target the liver or the spleen/bone marrow depending on coating density and peptide sequence.

4. Conclusions

We have demonstrated a simple and effective coating method to modify the function and toxicity of cationic gene delivery nanoparticles. These coatings expand the available parameter space by decoupling particle biophysical properties such as size and surface charge from properties intrinsic to the polymer such as DNA condensation and endosomal escape. We show that these electrostatic coatings have the potential to tune specific gene delivery away from the lungs and to the spleen and bone marrow or alternatively to liver cells. We anticipate that these electrostatic coatings could be used to coat a variety of particles to localize genes and other cargos to a various organs, tissues, and cells.

Acknowledgments

REFERENCES

1. Clayman GL, el-Naggar AK, Lippman SM, Henderson YC, Frederick M, Merritt JA, et al. Adenovirus-mediated p53 gene transfer in patients with advanced recurrent head and neck squamous cell carcinoma. J Clin Oncol 1998;16:2221–32. [PubMed: 9626224]

2. Ndoye A, Dolivet G, Hogset A, Leroux A, Fifre A, Erbacher P, et al. Eradication of p53-mutated head and neck squamous cell carcinoma xenografts using nonviral p53 gene therapy and photochemical internalization. Mol Ther 2006;13:1156–62. [PubMed: 16564229]

3. Manno CS, Pierce GF, Arruda VR, Glader B, Ragni M, Rasko JJ, et al. Successful transduction of liver in hemophilia by AAV-Factor IX and limitations imposed by the host immune response. Nat Med 2006;12:342–7. [PubMed: 16474400]

4. Park TG, Jeong JH, Kim SW. Current status of polymeric gene delivery systems. Adv Drug Delivery Rev 2006;58:467–86.

5. Thomas CE, Ehrhardt A, Kay MA. Progress and problems with the use of viral vectors for gene therapy. Nat Rev Genet 2003;4:346–58. [PubMed: 12728277]

6. Putnam D. Polymers for gene delivery across length scales. Nat Mater 2006;5:439–51. [PubMed: 16738681]

7. Pack DW, Hoffman AS, Pun S, Stayton PS. Design and development of polymers for gene delivery. Nat Rev Drug Discov 2005;4:581–93. [PubMed: 16052241]

8. Green JJ, Zugates GT, Tedford NC, Huang Y, Griffith LG, Lauffenburger DA, et al. Combinatorial modification of degradable polymers enables transfection of human cells comparable to adenovirus. Adv Mater 2007;19:2836–42.

9. Wood KC, Azarin SM, Arap W, Pasqualini R, Langer R, Hammond PT. Tumor-targeted gene delivery using molecularly engineered hybrid polymers functionalized with a tumor-homing peptide. Bioconjug Chem 2008;19:403–5. [PubMed: 18189340]

10. Thomas M, Klibanov AM. Enhancing polyethylenimine's delivery of plasmid DNA into mammalian cells. Proc Natl Acad Sci U S A 2002;99:14640–5. [PubMed: 12403826]

11. Srinivasachari S, Liu Y, Prevette LE, Reineke TM. Effects of trehalose click polymer length on pDNA complex stability and delivery efficacy. Biomaterials 2007;28:2885–98. [PubMed: 17367850]

12. Alexis F, Pridgen E, Molnar LK, Farokhzad OC. Factors affecting the clearance and biodistribution of polymeric nanoparticles. Mol Pharm 2008;5:505–15. [PubMed: 18672949]

13. Ogris M, Walker G, Blessing T, Kircheis R, Wolschek M, Wagner E. Tumor-targeted gene therapy: strategies for the preparation of ligand-polyethylene glycol-polyethylenimine/DNA complexes. J Controlled Release 2003;91:173–81.

14. Kircheis R, Wightman L, Schreiber A, Robitza B, Rossler V, Kursa M, et al. Polyethylenimine/DNA complexes shielded by transferrin target gene expression to tumors after systemic application. Gene Ther 2001;8:28–40. [PubMed: 11402299]

15. Suh W, Han SO, Yu L, Kim SW. An angiogenic, endothelial-cell-targeted polymeric gene carrier. Mol Ther 2002;6:664–72. [PubMed: 12409265]

16. Kursa M, Walker GF, Roessler V, Ogris M, Roedl W, Kircheis R, et al. Novel shielded transferrin-polyethylene glycol-polyethylenimine/DNA complexes for systemic tumor-targeted gene transfer. Bioconjug Chem 2003;14:222–31. [PubMed: 12526712]

17. Trubetskoy VS, Wong SC, Subbotin V, Budker VG, Loomis A, Hagstrom JE, et al. Recharging cationic DNA complexes with highly charged polyanions for in vitro and in vivo gene delivery. Gene Ther 2003;10:261–71. [PubMed: 12571634]

18. Fuller JE, Zugates GT, Ferreira LS, Ow HS, Nguyen NN, Wiesner UB, et al. Intracellular delivery of core-shell fluorescent silica nanoparticles. Biomaterials 2008;29:1526–32. [PubMed: 18096220]

19. Green JJ, Chiu E, Leshchiner ES, Shi J, Langer R, Anderson DG. Electrostatic ligand coatings of nanoparticles enable ligand-specific gene delivery to human primary cells. Nano Lett 2007;7:874–9. [PubMed: 17362046]

20. Zugates GT, Peng W, Zumbuehl A, Jhunjhunwala S, Huang YH, Langer R, et al. Rapid Optimization of Gene Delivery by Parallel End-modification of Poly(beta-amino ester)s. Mol Ther 2007;15:1306–12. [PubMed: 17375071]

21. Anderson DG, Peng W, Akinc A, Hossain N, Kohn A, Padera R, et al. A polymer library approach to suicide gene therapy for cancer. Proc Natl Acad Sci U S A 2004;101:16028–33. [PubMed: 15520369]

22. Green JJ, Anderson DG, Langer R. A combinatorial polymer library yields insights into the field of non-viral gene delivery. Acc Chem Res 2007;41:749–59.

23. Dunn JC, Yarmush ML, Koebe HG, Tompkins RG. Hepatocyte function and extracellular matrix geometry: long-term culture in a sandwich configuration. FASEB J 1989;3:174–7. [PubMed: 2914628]

24. Green JJ, Chiu E, Leshchiner ES, Shi J, Langer R, Anderson DG. Electrostatic ligand coatings of nanoparticles enable ligand-specific gene delivery to human primary cells. Nano Lett 2007;7:874–9. [PubMed: 17362046]

25. Chollet P, Favrot MC, Hurbin A, Coll JL. Side-effects of a systemic injection of linear polyethylenimine-DNA complexes. J Gene Med 2002;4:84–91. [PubMed: 11828391]

26. Goula D, Benoist C, Mantero S, Merlo G, Levi G, Demeneix BA. Polyethylenimine-based intravenous delivery of transgenes to mouse lung. Gene Ther 1998;5:1291–5. [PubMed: 9930332]

27. Dash PR, Read ML, Barrett LB, Wolfert MA, Seymour LW. Factors affecting blood clearance and in vivo distribution of polyelectrolyte complexes for gene delivery. Gene Ther 1999;6:643–50. [PubMed: 10476224]

28. Zou SM, Erbacher P, Remy JS, Behr JP. Systemic linear polyethylenimine (L-PEI)-mediated gene delivery in the mouse. J Gene Med 2000;2:128–34. [PubMed: 10809146]

29. Dobrovolskaia MA, McNeil SE. Immunological properties of engineered nanomaterials. Nat Nanotechnol 2007;2:469–78. [PubMed: 18654343]

30. Morimoto K, Nishikawa M, Kawakami S, Nakano T, Hattori Y, Fumoto S, et al. Molecular weight-dependent gene transfection activity of unmodified and galactosylated polyethyleneimine on hepatoma cells and mouse liver. Mol Ther 2003;7:254–61. [PubMed: 12597914]

31. Popielarski SR, Hu-Lieskovan S, French SW, Triche TJ, Davis ME. A nanoparticle-based model delivery system to guide the rational design of gene delivery to the liver. 2. In vitro and in vivo uptake results. Bioconjug Chem 2005;16:1071–80. [PubMed: 16173782]

32. Zhang XQ, Wang XL, Zhang PC, Liu ZL, Zhuo RX, Mao HQ, et al. Galactosylated ternary DNA/polyphosphoramidate nanoparticles mediate high gene transfection efficiency in hepatocytes. J Controlled Release 2005;102:749–63.

33. Zanta MA, Boussif O, Adib A, Behr JP. In vitro gene delivery to hepatocytes with galactosylated polyethylenimine. Bioconjug Chem 1997;8:839–44. [PubMed: 9404656]

34. Zugates, GT. Ph.D. Thesis. Massachusetts Institute of Technology; 2007. Synthesis and Chemical Modification of Degradable Polymers to Enhance Gene Delivery.

35. Rahman YE, Cerny EA, Patel KR, Lau EH, Wright BJ. Differential uptake of liposomes varying in size and lipid composition by parenchymal and kupffer cells of mouse liver. Life Sci 1982;31:2061–71. [PubMed: 7176810]

36. Nagayama S, Ogawara K, Fukuoka Y, Higaki K, Kimura T. Time-dependent changes in opsonin amount associated on nanoparticles alter their hepatic uptake characteristics. Int J Pharm 2007;342:215–21. [PubMed: 17566676]
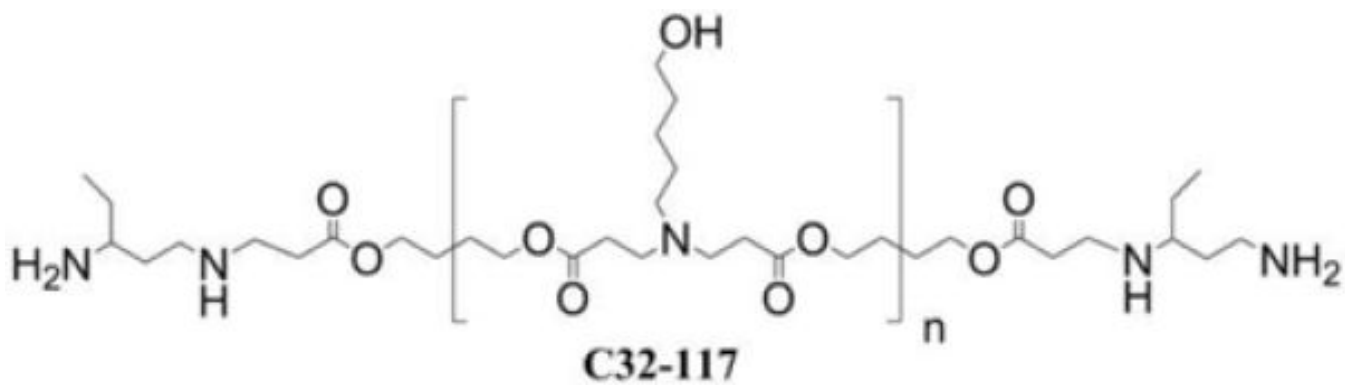
Figure 1. Polymer structure of C32–117
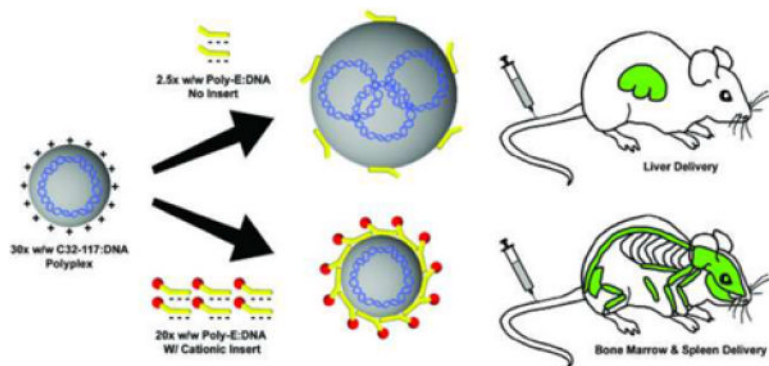Ends of the polymer can be in either of the two configurations shown.

Figure 2. Electrostatic coatings applied to cationic nanoparticles
Cationic nanoparticles are formed by first complexing poly (β-amino ester) C32–117 with plasmid DNA at a 30:1 polymer:DNA weight/weight ratio (w/w). These nanoparticles are then coated with poly(glutamic acid)-based peptides (poly-E or poly-E-cat) at 2.5:1–20:1 peptide:DNA w/w. Variation in peptide w/w tunes the biophysical properties of the nanoparticles and subsequent localization of gene delivery by the nanoparticles *in vivo*.
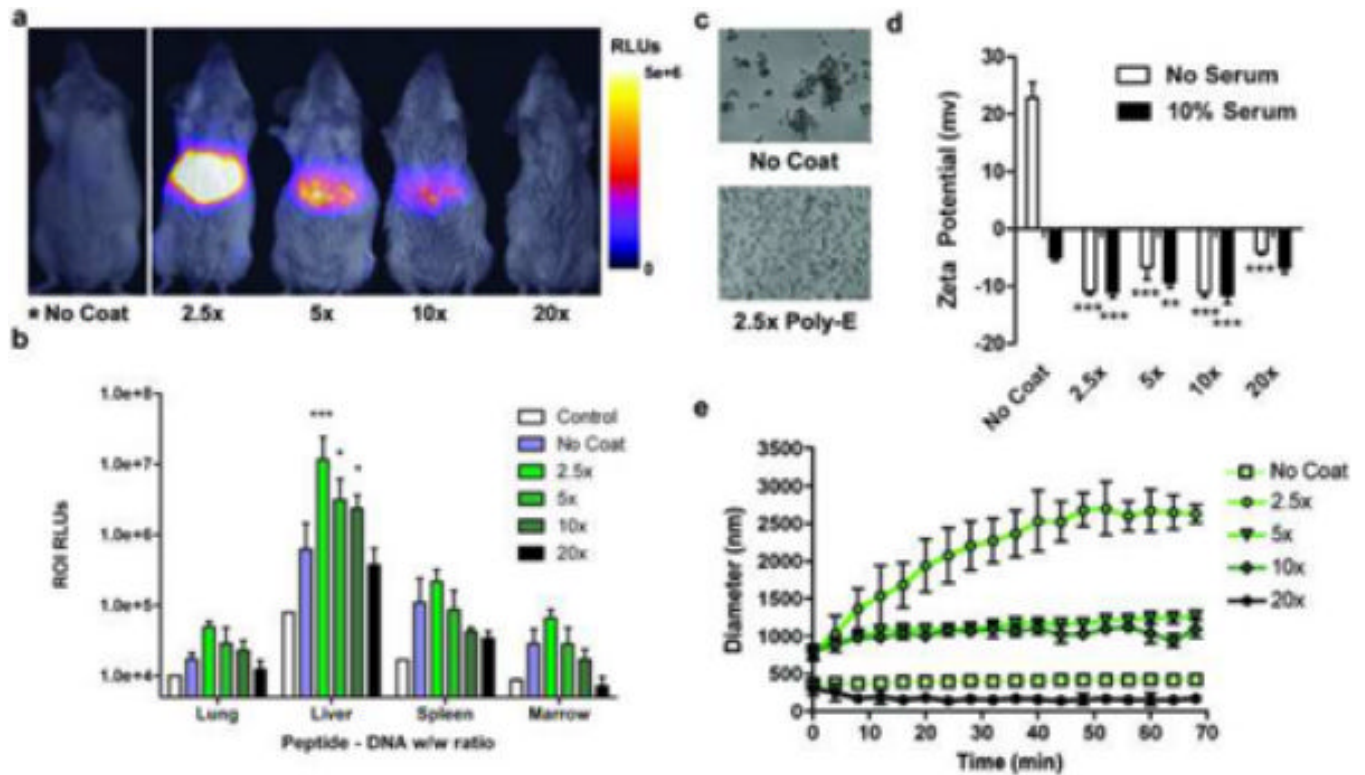
Figure 3. Effect of poly-E coatings on the biophysical and functional properties of gene delivery nanoparticles
a) Whole mouse bioluminescence imaging of mice injected with 50 μg of pCMV-LUC plasmid DNA complexed with C32–117 and coated with 2.5:1–20:1 w/w poly-E peptides. b) Luciferase expression in lungs, liver, spleen, and femur bone marrow demonstrates specific liver delivery by poly-E peptide coated nanoparticles (* = p<0.05, *** = p<0.001 for each coating as compared to uncoated particles, two-way ANOVA) c) C32–117 nanoparticles aggregate freshly isolated erythrocytes when mixed *in vitro*, a contributor to toxicity, while 2.5:1 w/w poly-E coated nanoparticles have no effect. d) Non-coated particles have a positive zeta potential that becomes negative when incubated in serum. The adsorption of poly-E coatings shifts the nanoparticle surface potential to negative in serum and serum free buffer (** = p<0.01, *** = p<0.001 for each coating as compared to uncoated particles, two-way ANOVA). e) Dynamic light scattering shows coating dependent changes in particle size that coincide with liver delivery function.
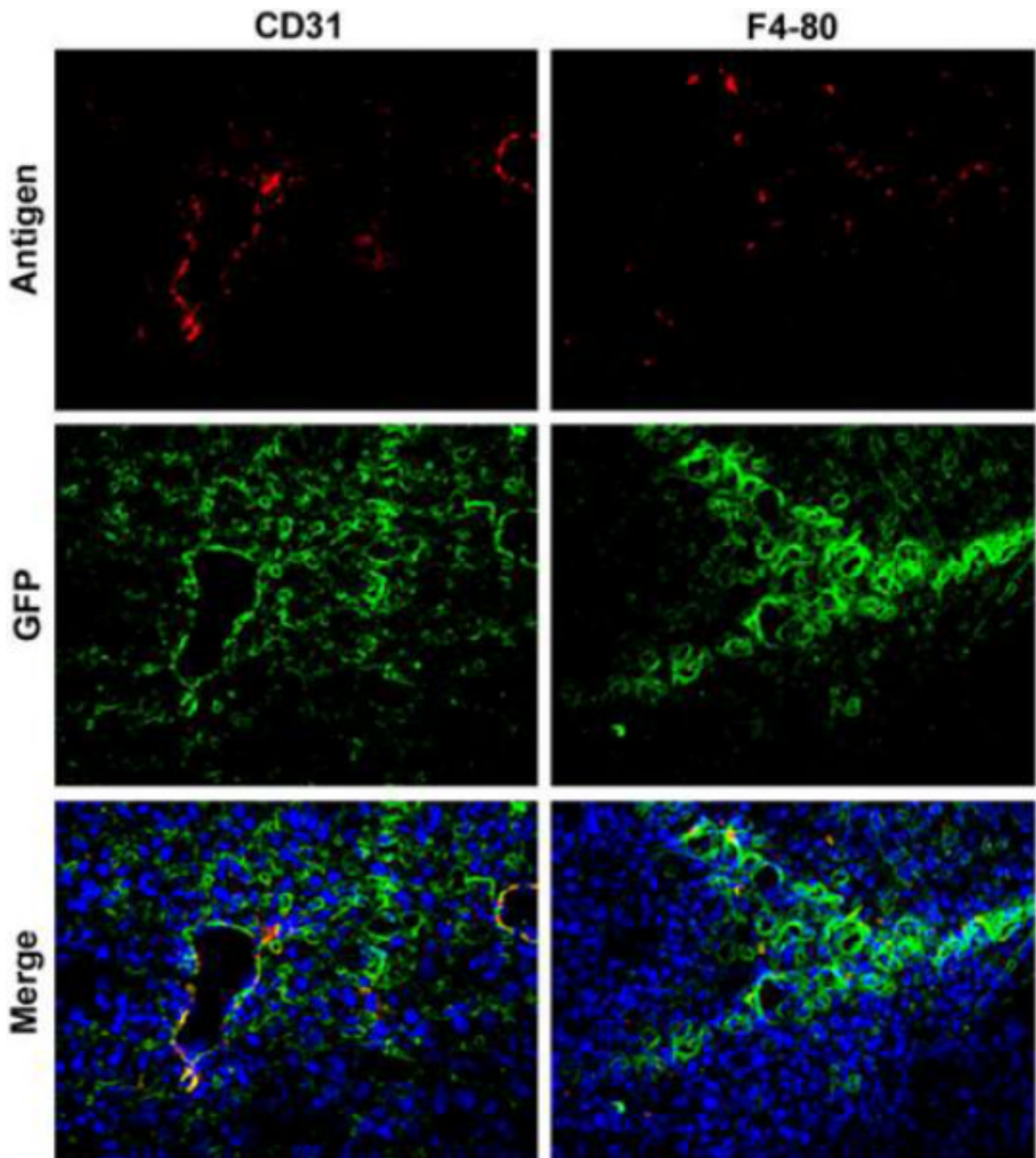
Figure 4. Analysis of the liver cell targeting nanoparticles
Histological analysis of mouse livers 6 hrs post injection of 2.5 w/w poly-E coated pEGFP-N1 gene delivery particles show gene expression in both CD31 positive and negative vessels. GFP expression also colocalizes in Kupffer cells (F4–80) near vessel borders.
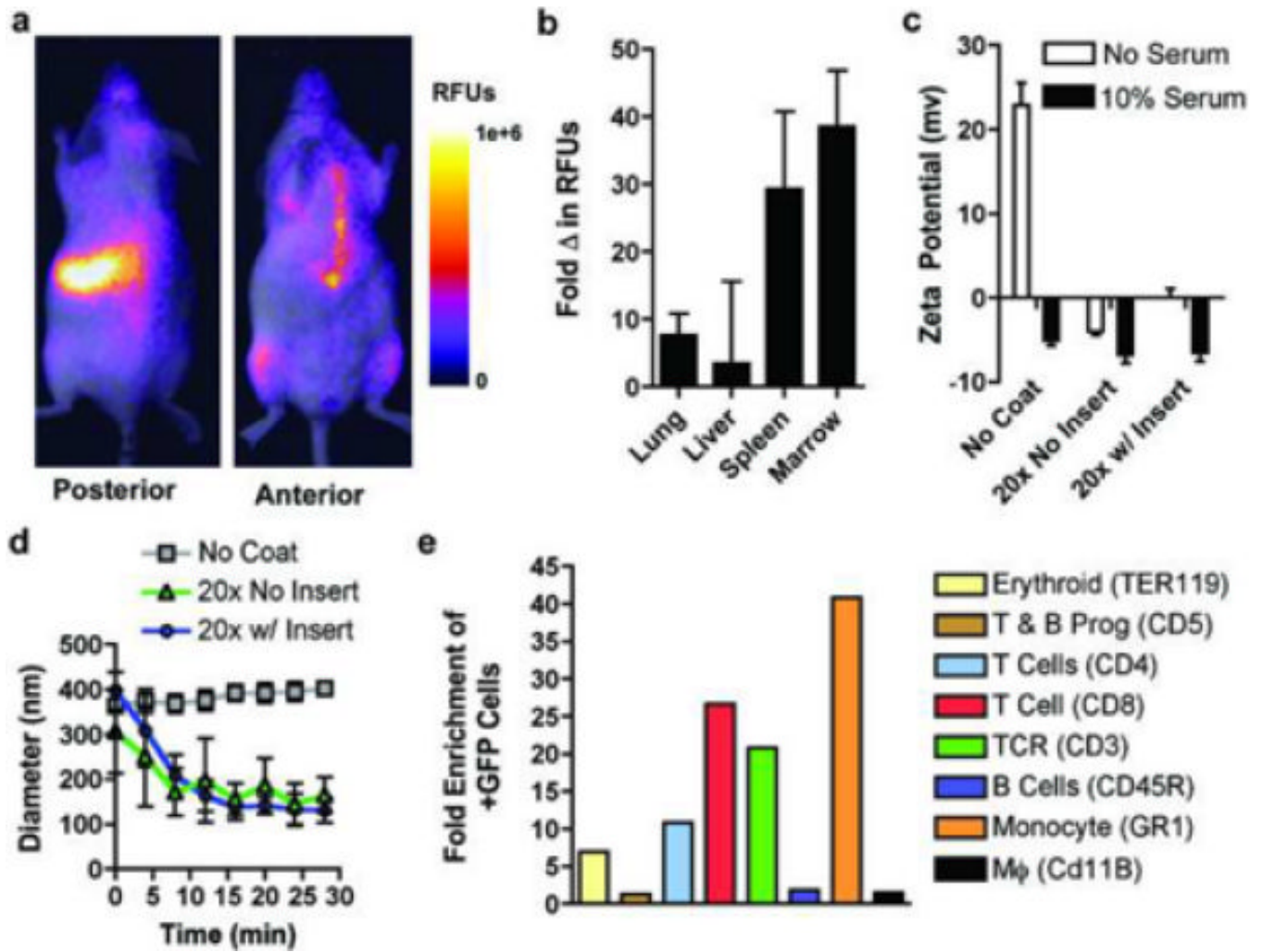
Figure 5. Introduction of cationic inserts inhigh-density poly-E coatings targets gene delivery particles to the bone marrow and spleen

a) Whole mouse bioluminescence imaging of mice injected with 50 μg of pCMV-LUC plasmid DNA complexed with C32–117 and coated with 20 w/w poly-E-cat peptides shows gene expression localized to the spleen and bone marrow rich structures. b) Fold enhancement in luciferase expression by nanoparticles coated with poly-E-cat peptides (w/ cationic insert sequence) relative to poly-E coatings (without insert). c) Zeta potential of 20:1 w/w poly-E-cat (w/insert) coated nanoparticles is neutral in serum-free media, whereas poly-E coated nanoparticles are negatively charged and uncoated particles are strongly positively charged. After incubation in serum, particle charges of each formulation are weakly negative. d) Dynamic light scattering shows that 20:1 w/w poly-E coatings and poly-E-cat coatings both form 200 nm nanoparticles in the presence of serum. The cationic sequence insert has negligible effect on nanoparticle size. The coated particles are significantly smaller than the uncoated particles (p<0.01 for both "no insert" and "insert" by two-way ANOVA and the Bonferroni post-test) e) Flow cytometry analysis of bone marrow cells from a mouse injected tail-vein with GFP-encoding nanoparticles coated with 20:1 w/w poly-E-cat peptides. GFP expression relative to the whole population of bone marrow cells is enriched in monocyte and T-cell lineage cells.
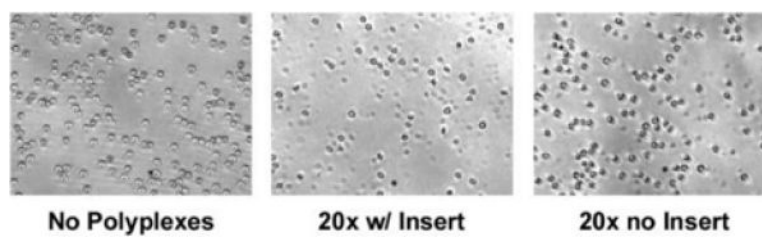
Figure 6. C32–117 nanoparticles coated with 20:1 w/w poly-E-cat (w/ insert) and 20:1 w/w poly-E (no insert) peptides do not aggregate freshly isolated erythrocytes when mixed *in vitro*
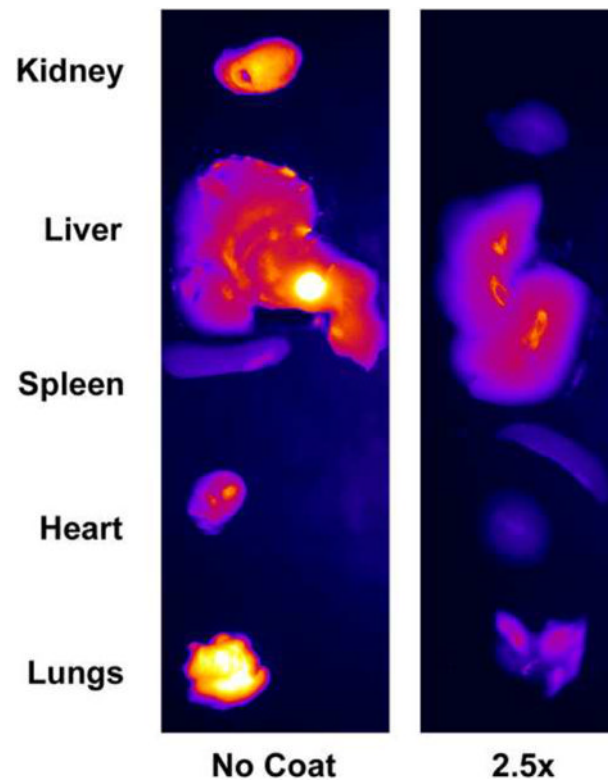
Figure 7. Near infrared fluorophore labeled DNA accumulates in the lungs of mice injected tail-vein with a lethal dose (50 μg DNA) of non-coated particles
Mice injected with the same dose of 2.5 w/w poly-E coated particles tolerate the injection well and show no lung accumulation when sacrificed at 24 hr post injection.